

## RESEARCH ARTICLE

# Comparative Evaluation of Activated and Non-Activated Sunflower Seed Husks surface for removal of Toxic Industrial Dyes

Uday Abdul-Reda Hussein<sup>1</sup>, Hayder Hamid Abbas Al-Anbari<sup>2</sup>, Turki Meften Saad<sup>3</sup>, Abed J. Kadhim<sup>4</sup>, Fadhil M. Abid<sup>5</sup>, Aseel M. Aljeboree<sup>6</sup>, Ayad F. Alkaim<sup>6\*</sup>

<sup>1</sup> Department of pharmaceutics, College of Pharmacy, University of Al-Ameed, Iraq

<sup>2</sup> Ahl Al bayt University/ College of pharmacy/ Kerbala/ Iraq

<sup>3</sup> Department of Medical Laboratories, College of health & medical Technology, Sawa University, Almuthana, Iraq

<sup>4</sup> Department of Medical Laboratories Technology, AL-Nisour University College, Baghdad, Iraq

<sup>5</sup> Al-Hadi University College, Baghdad, 10011, Iraq

<sup>6</sup> Department of chemistry, college of sciences for women, University of Babylon, Iraq

\*Corresponding author: Ayad F. Alkaim, alkaimayad@gmail.com

### ARTICLE INFO

Received: 24 September 2025

Accepted: 01 November 2025

Available online: 04 January 2025

### COPYRIGHT

Copyright © 2026 by author(s).

*Applied Chemical Engineering* is published by Arts and Science Press Pte. Ltd. This work is licensed under the Creative Commons Attribution-NonCommercial 4.0 International License (CC BY 4.0).

<https://creativecommons.org/licenses/by/4.0/>

### ABSTRACT

The adsorption of the potentially toxic industrial dyes, Acid Red 18 (AR18), Acid Yellow 23 (AY23), Reactive Yellow 84 (RY84), and Reactive Black 5 (RB5). was assessed in this work using non-activated and activated sunflower seed husks as environmentally sound adsorbents. Hydrochloric, phosphoric and sulfuric acids activated the sunflower seed husk, and the best chemical activation method was determined by surface morphology and the adsorption performance. The optimal temperature for thermal treatment to convert biomass into activated carbon has been established. The structural and chemical characteristics of the adsorbents were investigated by the characterization techniques such as Field Emission Scanning Electron Microscopy (FESEM), Energy Dispersive X-ray Spectroscopy (EDX), Transmission Electron Microscopy (TEM), and Fourier-Transform Infrared Spectroscopy (FTIR). The percentage removals of Reactive Yellow, Reactive Black 5, Acid Red, and Acid Yellow 23 were determined to be (95.02%, 90.00%, 85.00% and 70.00% for the acid-activated sunflower seed husks. These values were significantly higher than the adsorption capacities of non-activated husks, 80.02%, 75.27%, 55.70%, and 45.00%, respectively, for the corresponding dyes. The findings demonstrate an improvement in the properties of acid-activated sunflower seed husks in the adsorption of dyes (Reactive Black 5 and Acid Red), reflecting the influence of acid activation on expansion of the specific surface area and availability of functional groups. Adsorption efficiency was highest under acidic conditions due to enhanced electrostatic attraction between the adsorbent surface and dye molecules. Reactive dyes showed greater sensitivity to pH variation, with efficiency dropping sharply in alkaline media. In contrast, Acid dyes—particularly Acid Yellow—retained higher performance across the pH range, indicating additional binding mechanisms beyond electrostatic interactions.

**Keywords:** Activated carbon; Sunflower seed husks; Dyes, Removal; Adsorption

# 1. Introduction

The discharge of dye effluents from various industrial processes has become a significant environmental concern, particularly due to the widespread use of synthetic dyes in the textile, leather, paper, and cosmetics industries [1,2]. Such dyes, especially those of an azo and reactive type, possess complicated organic aromatic molecular structures that confer good stability, nonbiodegradability and strong resistances to light, heat and microbial attacks. Therefore, their effluent in water bodies not only produces intense colouration of water, but it also contains toxic, cancerogenic and mutagenic compounds with high-risk hazards to impact life in water bodies and human health [3].

However, conventional wastewater treatment processes, such as coagulation-flocculation, membrane filtration, and biological decomposition, do not effectively remove dyes due to their extremely poor biodegradability and recalcitrance in chemical terms. In this regard, adsorption has emerged as a highly efficient, cost-effective, and eco-friendly method for dye removal. The adsorption process efficiency is significantly influenced by the nature of the adsorbent material; hence, there is continuous interest in exploring new and cost-effective, environment-friendly, and high-capacity adsorbents obtained from agrowastes and industrial wastes [4-9]. Of these, lignocellulose biomass material, such as sunflower seed husk, has excellent potential due to its wide availability, sustainability, and adjustable surface properties. The adsorptive capacity of such biomass could be substantially increased by surface activation, especially through acid treatments that increase the surface area and porosity, and the accessibility of the functional groups, rendering them suitable for dye remediation applications [10-11].

## 2. Experimental part

### 2.1. Sunflower seed shell

The study was conducted with the seed shells of sunflower (*Helianthus annuus* L.) collected in a supermarket in Iraq. The contents of individual polysaccharides in the hulls are as follows: hemicellulose 24.0%, cellulose 42.7%, and lignin 23.2%.

### 2.2. Dyes

The study employed anionic dyes, which are commonly used in the textile industry, including Acid Red 18 (AR18), Acid Yellow 23 (AY23), Reactive Yellow 84 (RY84), and Reactive Black 5 (RB5). Dyes originated from a dye production plant, specifically a textile dye. Iraq -Hilla, their characteristics are presented in Table 1.

**Table 1.** Characteristics of dyes utilized in the study

Name Dye	Acid Yellow 23	Acid Red 18	Reactive Yellow 84	Reactive Black 5
Structural formula				
Dye type	Anionic (acid)	Anionic (acid)	Anionic (reactive)	Anionic (reactive)
Chemical formula	C <sub>16</sub> H <sub>9</sub> N <sub>4</sub> Na <sub>3</sub> O <sub>9</sub> S <sub>2</sub>	C <sub>20</sub> H <sub>11</sub> N <sub>2</sub> Na <sub>3</sub> O <sub>10</sub> S <sub>3</sub>	C <sub>18</sub> H <sub>14</sub> Cl <sub>2</sub> N <sub>8</sub> Na <sub>2</sub> O <sub>9</sub> S <sub>2</sub>	C <sub>26</sub> H <sub>25</sub> N <sub>5</sub> O <sub>19</sub> S <sub>6.4</sub> Na
λ <sub>max</sub>	420nm	510 nm	450 nm	590 nm

Molecular weight	534 g/mol	604 g/mol	628 g/mol	991 g/mol
------------------	-----------	-----------	-----------	-----------

### 2.3.Preparation of sunflower seed shells (SSS)

Sunflower seed shells (SSS) were initially washed thoroughly with distilled water to remove surface impurities, followed by oven drying and mechanical grinding using a laboratory-scale electric grinder. The ground material was subsequently sieved to obtain particle sizes ranging from 2 to 4 mm using a 5 mm mesh sieve. The sieved fractions were then subjected to chemical pretreatment by immersion in various acidic solutions, including hydrochloric acid (HCl), phosphoric acid ( $H_3PO_4$ ), nitric acid ( $HNO_3$ ), and 2 M sulfuric acid ( $H_2SO_4$ ), for 24 hours under ambient conditions. As shown in Figure 1.

Following acid treatment, the shells were filtered and rinsed repeatedly with distilled water until a neutral pH was achieved. Among the acids tested, hydrochloric acid demonstrated the most effective activation performance. The acid-treated shells were then immersed in a sodium hydroxide (NaOH) solution for an additional 24-hour period to enhance surface modification. After alkaline treatment, the material was again filtered and washed with distilled water to remove any residual alkali. The prepared and chemically modified sunflower seed shells were then stored in distilled water before further characterization and use in adsorption experiments.

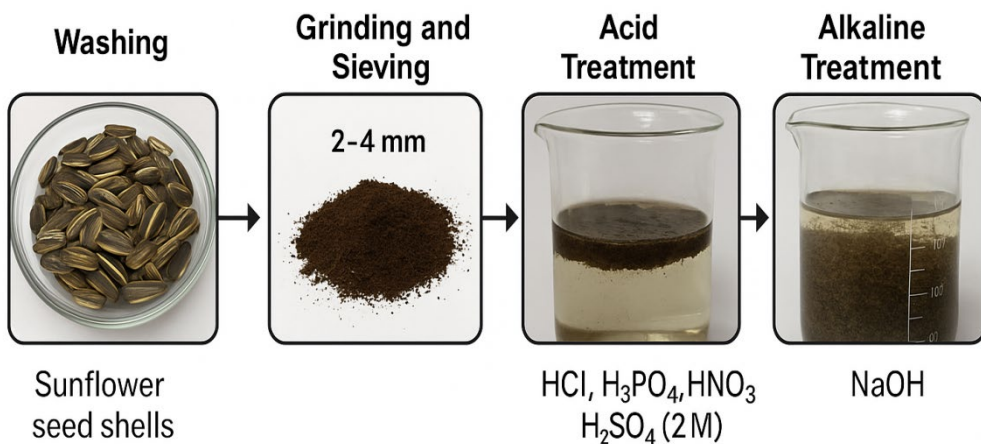


**Figure 1.** Preparation of Sunflower Seed Shells (SSS)

### 2.4.Activation of sunflower seed shells using hydrochloric acid

A total of 100 grams of sunflower seed shells were placed into a 300 mL conical flask, to which concentrated hydrochloric acid solution (>99%) was added to initiate chemical activation. The mixture was left to stand for 24 hours at room temperature to allow sufficient interaction between the acid and the biomass. After the treatment period, the shells were thoroughly filtered and repeatedly rinsed with distilled water to eliminate any residual acid and neutralize the surface. Subsequently, the acid-treated shells were subjected to thermal activation by heating in a muffle furnace at four different temperatures—200°C, 300°C, 400°C, and 500°C—for a duration of 2 hours each. This carbonization process facilitated the formation of activated carbon with enhanced porosity and surface area. After cooling, the samples were again washed with distilled water to remove any remaining impurities, then dried and stored in airtight containers for further characterization and adsorption experiments.

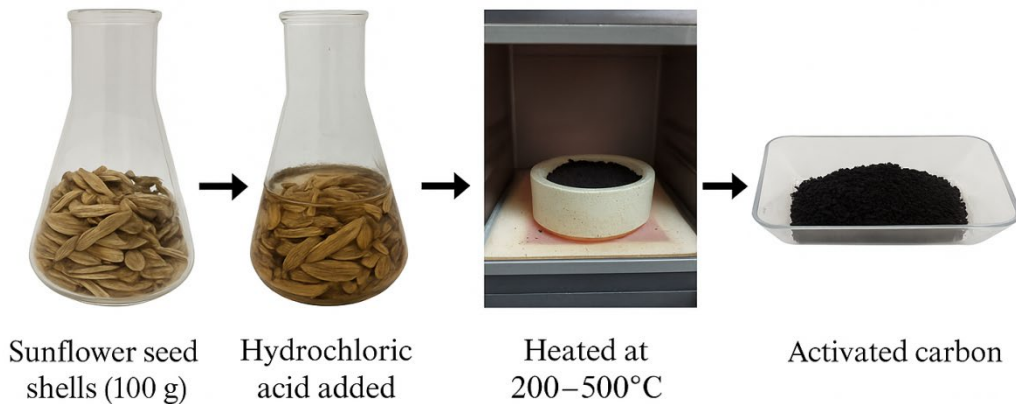


**Figure 2.** Activation of Sunflower Seed Shells Using Hydrochloric Acid

## 2.5. Adsorption study

The stock solutions of Acid Red 18 (AR18), Acid Yellow 23 (AY23), Reactive Yellow 84 (RY84), and Reactive Black 5 (RB5). dye were diluted to the desired concentrations to prepare a standard dye solution, from 100 mg/L. For batch mode adsorption tests, 100 mL conical flasks were filled with 0.08 g of adsorbent and 100 mL of the prepared dye solution, maintaining an initial pH of 6. Using a mechanical shaker, the flasks were shaken at 120 rpm for 1 hour at a temperature of 25±2°C. After agitation, centrifugation was performed to separate the adsorbent from the adsorbate. The Acid Red 18 (AR18), Acid Yellow 23 (AY23), Reactive Yellow 84 (RY84), and Reactive Black 5 (RB5) and, Acid Red 18 (AR18). The acid yellow acid, Red, Reactive Yellow 86, and Reactive Black 5 dye content in the supernatant was then measured using spectrophotometry at wavelengths of 420 nm, 510 nm, 450 nm, and 590 nm. Experiments were conducted at a constant dye concentration of 100 mg/L, with varying clay dosages ranging from 0.08g per 100 mL, to investigate the effect of AC dosage on the percentage of dye elimination.

$$E \% = \frac{C_o - C_e}{C_o} \times 100 \quad (1)$$

where  $C_o$  (mg/L) is the initial concentration of dyes, and  $C_e$  (mg/L) is the concentration of dyes at equilibrium.

## 2.6. SEM for Raw Sunflower Seed Shells before and after acid Activation

The surface morphology of the untreated sunflower seed shells was observed at 100,000× under SEM micrograph in Figure 3a. The image is inhomogeneous and relatively aggregated, with particles adhered to the surface that do not have a regular shape. Variation in the types of both granulofibrous components is due to the lignocellulosic nature of the biomass, which predominantly consists of cellulose, hemicellulose, and lignin. The surface appears rough and irregular, with few visible porosities or open pore structures. This denotes the small surface area and little adsorption capacity of the raw material before activation. The morphological features indicate that the surface of the material is devoid of any properly developed micropores or mesopores, which is very important for adsorption in the case of activated carbon. This starting morphology serves as a reference point for comparing against post-activation materials, which, unsurprisingly, undergo drastic structural alterations, including changes in texture, porosity, and surface area, induced by acid treatment and thermal treatment [12-13].

The surface morphology of the sunflower seed hulls after HCl-chemical activation and carbonization was observed by SEM in Figure 3b . The topography of the surface is radically altered concerning that of the raw material, where a more open and disordered network of fine particles and stretched structures is observed. More roughness texture and higher fragmentation were observed in the sonicated sample (CAN),

indicative of lignocellulosic component disruption, which is likely to occur during thermal processing as well. Many kinds of micropores and mesopores can be generally scattered throughout it, promoting the available surface area, which is essential for adsorption purposes. This porous structure is formed by the chemical etching in the acid treatment process and the outgassing in carbonization, and altogether has developed the internal pore network. The enhanced textural properties of this image indicate its potential as an adsorbent, in which the activated carbon prepared from sunflower seed shells could find potential applications for environmental protection purposes, such as the removal of industrial dyes or heavy metals from aqueous systems [14-15].

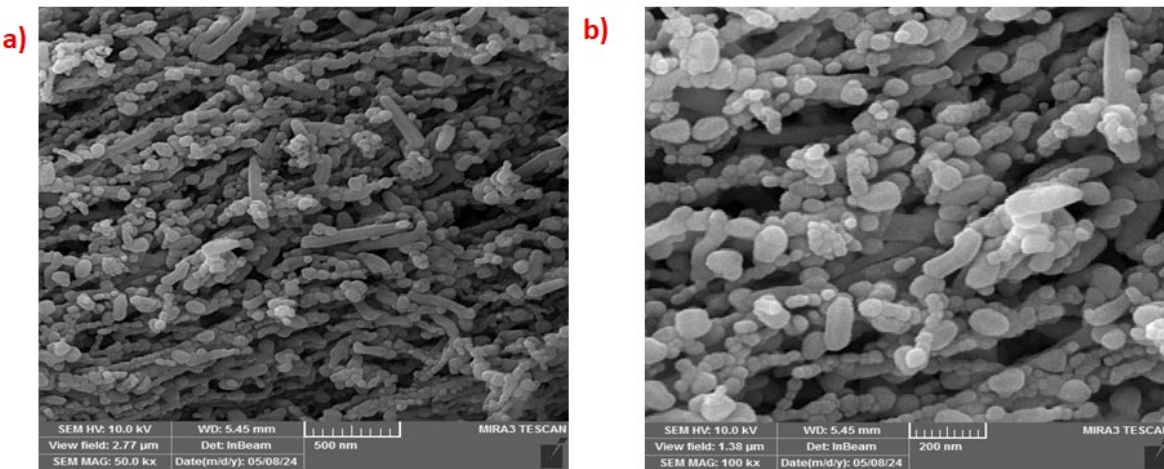


**Figure 3.** SEM Analysis of a) Sunflower Seed Shells , b) Sunflower Seed Shells After Acid Activation and Carbonization

## 2.7. SEM Analysis of Activated Sunflower Seed Shells After Adsorption of Acid Red 18 (AR18), Acid Yellow 23 (AY23) dyes

Figure 4a SEM image at 100,000 $\times$  of the surface morphologies of hydrochloric acid-activated sunflower seed shells after the adsorption of Acid Yellow. This surface is more homogeneously covered and is destroyed in compacted, partially coated with globular and randomly shaped deposits than the prior adsorbed active sample.

Such morphological characteristics of the adsorbents imply that the dyes were effectively adsorbed. The pores of high roughness and thickness appear lighter or darker than well-pores, as they are blocked or filled by the dye molecule, which favours the immobilisation of dye molecules on adsorbent surfaces. The obscured inner pores and uneven surface with adherent dye particles provide further evidence that the adsorptive bond between the dye and active surface functional groups is illustrated. This microstructural evidence endorses the adsorption mechanism, revealing a highly efficient removal of Acid Yellow dye molecules on the prepared activated carbon. This is the reason why the distorting surface morphology after adsorption is indicative of the applicability of this bio-based adsorbent to real wastewater treatment and dye removal [12].

The SEM image, at 100,000 $\times$  magnification (Figure 4b), shows the surface morphology of acid-activated sunflower seed shell-based carbon after the adsorption of Acid Red dye. The surface morphology is significantly altered compared with the pre-adsorption shape with some portion of the surface covered by dye particles.

The surface of activated carbon becomes more crowded with the presence of smaller pores and voids occupied either wholly or partially by dye aggregates. The rather densely adsorbed material has covered the

initially well-defined porous network. This morphological change indicates that the Acid Red dye molecules were successfully attached to the adsorbent's surface through various types of interactions, including electrostatic attractions, hydrogen bonding, and  $\pi$ - $\pi$  stacking between the planar aromatic groups of the dye and the carbon surface. These results indicate that both the functionalized sites and porous structures are involved in the adsorption of dye contaminants, further demonstrating the applicability of chemically activated sunflower seed shells for removing dyes in wastewater treatment processes<sup>[16-17]</sup>.

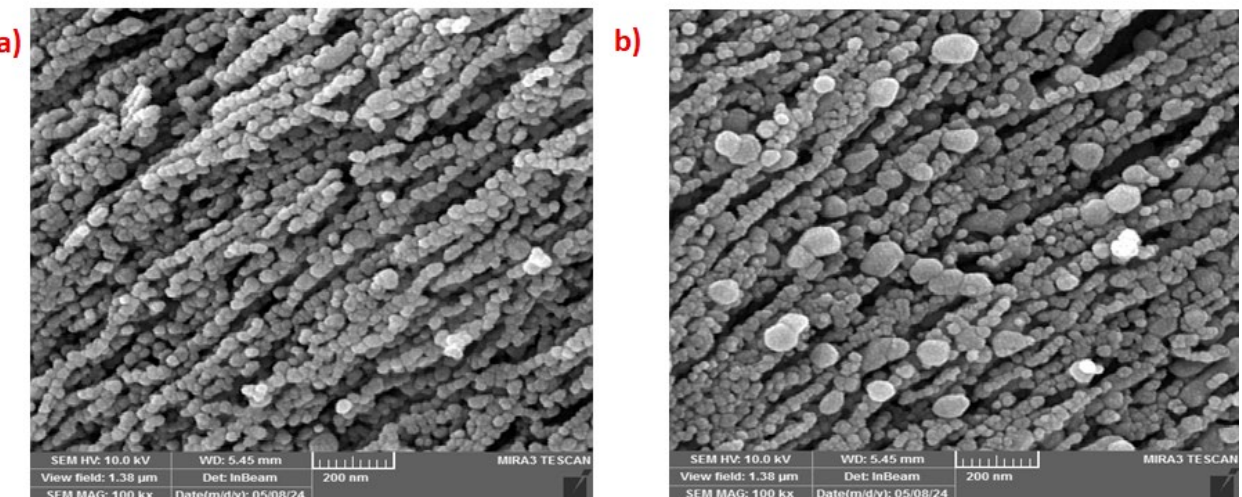


**Figure 4.** SEM Analysis of Activated Sunflower Seed Shells After Adsorption of a) Acid Yellow 23 (AY23), b) Acid Red 18 (AR18) Dyes

## 2.8. SEM Analysis of Activated Sunflower Seed Shells After Adsorption of Reactive Yellow 84 (RY84), and Reactive Black 5 (RB5) Dyes.

This SEM image, acquired at 100,000 $\times$  magnification Figure 5a, presents the surface morphology of activated sunflower seed shells following the adsorption of Reactive Yellow 86 dye. The surface exhibits a densely coated structure with uniformly distributed adsorbed particles across the carbon framework.

The fibrous architecture of the substrate remains partially visible, but a considerable amount of dye appears to have adhered to the surface. This is evidenced by the thickened texture and the granular accumulation that conceals many of the previously open pore structures observed in the unadsorbed sample. The agglomerated formations suggest strong interactions between the dye molecules and the activated carbon surface, likely facilitated by ion exchange, electrostatic interactions, and surface functional groups created during the acid activation process. The adequate surface coverage seen in this micrograph confirms the high adsorption affinity of the prepared material for Reactive Yellow 23, highlighting its potential for application in treating dye-laden industrial effluents<sup>[18]</sup>.

The SEM image, taken at 100,000 $\times$  magnification, shows the surface morphology of hydrogen chloride-activated sunflower seed shell-based carbon after exposure to Reactive Black 5 dye. The structure exhibits an ample surface coverage, with the accumulation of adsorbate material along the fibrous network of the carbon support being apparent in Figure 5b.

The pores and microstructures are partially or entirely covered concerning the pre-adsorption surface, suggesting the effective adsorption of the dye molecules. The fact that the particulate material was spread evenly and closely packed on the substrate indicates strong interactions between the dye and the functionalized carbon surface, which are most likely mediated through hydrogen bonding, electrostatic interactions, or  $\pi$ - $\pi$  interactions among aromatic moieties. The structure of the fibrous framework remains intact, while the surface presents low porosity and high mass density, verifying the Reactive Black 5 adsorption. These morphological observable characteristics further confirm the suitability of the activated

sunflower seed shell material as a high-capacity adsorbent for removing reactive dyes in wastewater treatment [19-20].

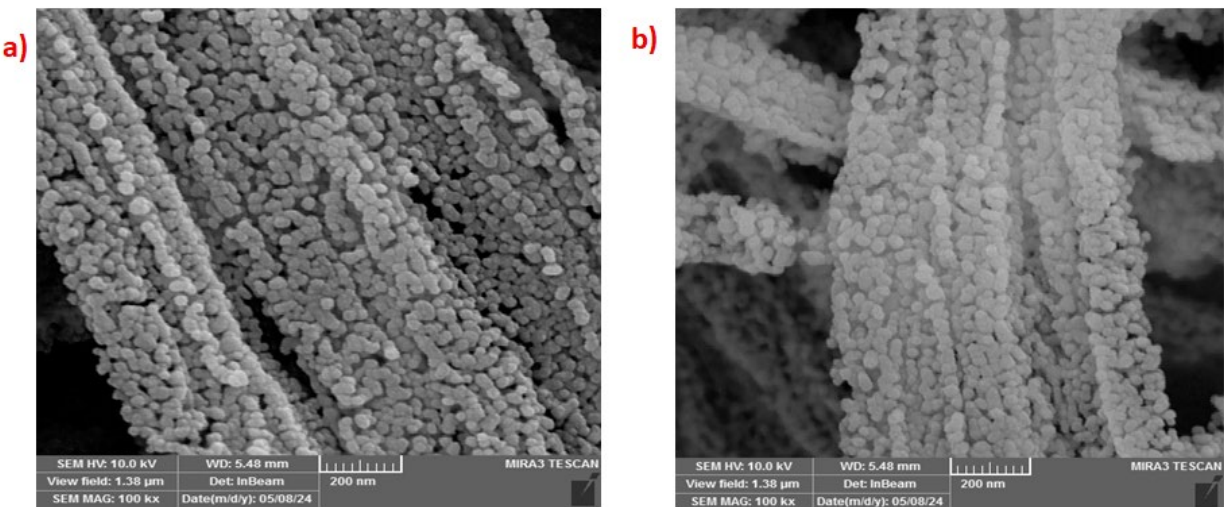


**Figure 5.** SEM Analysis of Activated Sunflower Seed Shells After Adsorption of a) Reactive Yellow 84 (RY84), and b) Reactive Black 5 (RB5) Dyes.

## 2.9. TEM analysis of raw (activated and unactivated) sunflower seed shells

The Transmission Electron Microscopy (TEM) image displays a thin, sheet-like fragment of unactivated sunflower seed shell biomass at the nanoscale, with a reference scale of 60 nm. The observed structure appears dense and relatively homogeneous, with limited contrast variation, suggesting a compact and undeveloped internal architecture typical of raw lignocellulosic materials Figure 6 a .

The absence of distinct pores or disordered regions indicates that the material has not yet undergone any physical or chemical activation. This compact morphology corresponds to the native organisation of cellulose, hemicellulose, and lignin—key structural biopolymers in plant biomass. These tightly bound components contribute to the low surface area and poor adsorption performance commonly observed in untreated agricultural waste. This microstructural characterisation serves as a baseline reference for evaluating the morphological changes that occur upon acid activation and carbonisation, where the formation of porosity, surface defects, and structural irregularities significantly enhances adsorption capacity [21].

The microstructure of the sunflower seed shells after acid-assisted chemical activation, at a scale of 60 nm, is presented in Figure 6 b as an image from TEM . As opposed to the virgin material, the activated sample shows a rougher and less dense structure, characterized by the presence of porous and amorphous regions. Such modifications indicate the destruction of the original lignocellulosic matrix during acid treatment. The structure relaxation observed in them can be attributed to the partial degradation and elimination of hemicellulose and lignin-derived constituents through the activation process. This forms a larger, looser structure, increasing surface area and number of adsorption sites. Additionally, the rough, sponge-like texture in the picture indicates the creation of nano-scale pores and active surface functional groups, which provide prominent adsorption characteristics. Overall, the TEM image confirms that acid treatment results in a dramatic modification of the internal structure of the sunflower seed shells, rendering them more suitable for high-performance adsorbents in environmental remediation applications [22].

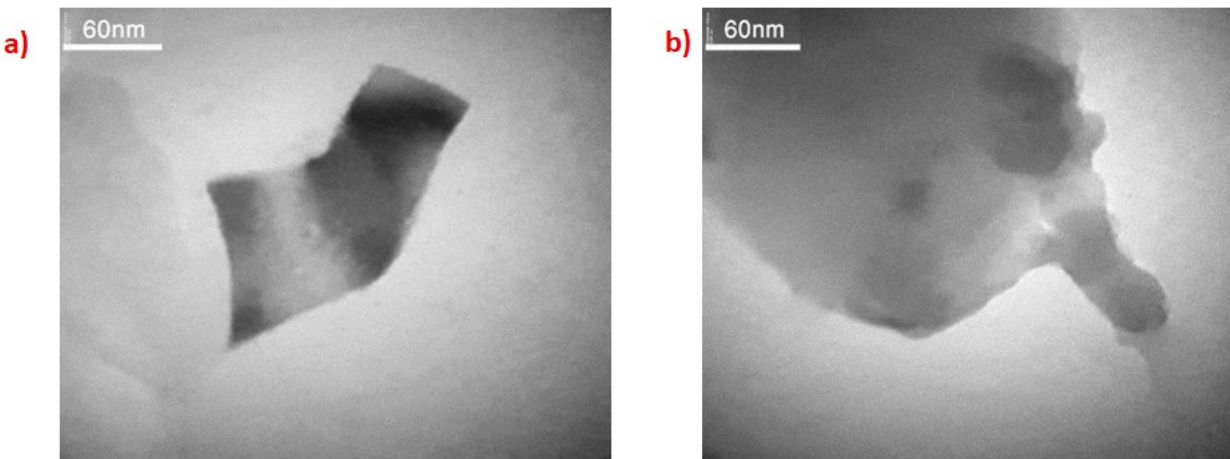


**Figure 6.** TEM Analysis of Raw a) Activated and b) Unactivated Sunflower Seed Shells

## 2.10. EDX investigation of carbon material derived from sunflower seed shell

The EDX spectrum of the sunflower seed shell after acid activation and carbonization is presented in Figure 7. The spectrum confirms the presence of C and O in the material, with their weight percentages being 75.1% C and 24.9% O, respectively. Elemental analysis reveals the carbon-rich nature of the treated biomass, indicating the successful preparation of the carbon adsorbent. The high level of carbon content is standard for lignocellulosic biomass-derived biochar and activated carbon, indicating the successful decomposition of non-carbon elements during pyrolysis and the accumulation of significant quantities of aromatic carbon structures. The oxygen is indicative of a plausible presence of oxygen-functional groups (e.g., hydroxyl, carbonyl and carboxyl groups), which are necessary for surface reactivity and interaction with polar pollutants such as dyes or heavy-metal species. The gold (Au) peaks can be seen at different energy levels, originated from the gold coating used in the sample for good conduction during SEM/EDX examination. These peaks are not native components of the sample and can therefore be removed from chemical analysis. The characterization by EDX indicates that the material has high carbon content and surface chemistry rich in oxygen functionalities, features that are desirable for adsorption in environmental remediation [23-24].

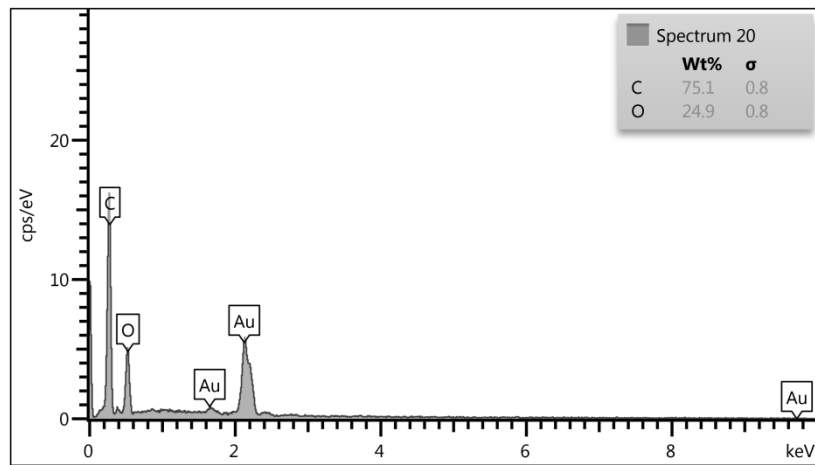


**Figure 7.** EDX Investigation of Carbon Material Derived from Sunflower Seed Shell

## 2.11. FTIR spectral features after dye adsorption

Following dye adsorption, the FTIR spectra of ACSS exhibited distinct changes corresponding to each dye Figure 8. For Reactive Black 5, the spectrum showed a noticeable reduction in the intensity of the O–H stretching band around  $3400\text{ cm}^{-1}$  and a shift in the C=O peak near  $1700\text{ cm}^{-1}$ , indicating strong hydrogen bonding and possible  $\pi$ – $\pi$  interactions with aromatic dye structures. In the case of Acid Yellow, a broadening of the O–H band and shifts in the C–O stretching region ( $1250$ – $1050\text{ cm}^{-1}$ ) were observed, suggesting electrostatic interactions and surface complexation. For Acid Red, the FTIR spectrum revealed decreased transmittance in both the O–H and C=O regions along with intensified peaks near  $1600\text{ cm}^{-1}$ , reflecting enhanced aromatic stacking and bonding through oxygenated functional groups. These spectral changes confirm the participation of hydroxyl, carbonyl, and ether groups in the adsorption process for all dyes [25–26].

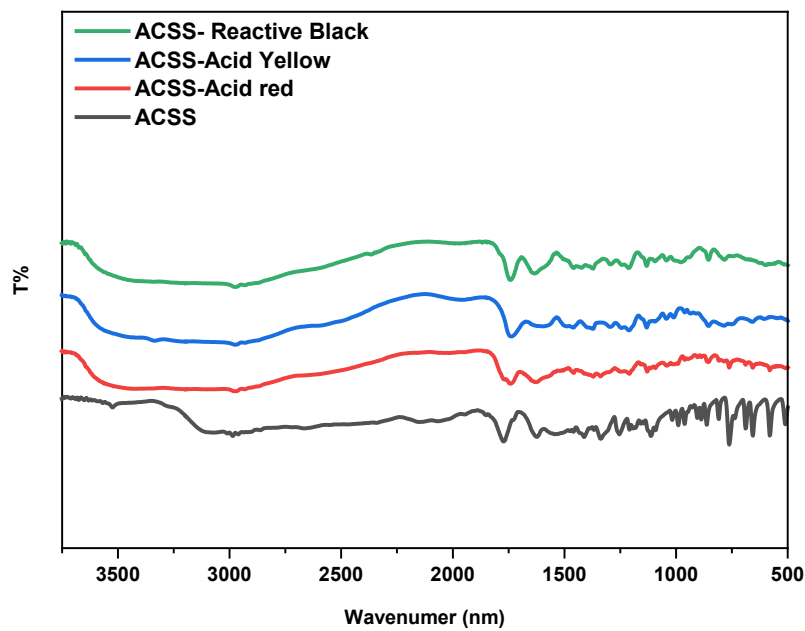


**Figure 8.** FTIR Analysis of Activated Carbon from Sunflower Seed Shells Before and after adsorption of dyes (\*Reactive Yellow 84 (RY84) didn't show pure FTIR in this study)

## 2.12. Acid activation of sunflower seed shells

Figure 9 illustrates the effect of different chemical activating agents—HCl,  $\text{H}_2\text{SO}_4$ ,  $\text{HNO}_3$ , and  $\text{H}_3\text{PO}_4$ —on the adsorption efficiency (E%) of activated carbon derived from sunflower biomass. Among the tested acids, HCl activation produced the highest adsorption efficiency, reaching approximately 88%, followed by  $\text{H}_2\text{SO}_4$  with slightly lower performance.  $\text{HNO}_3$  showed moderate efficiency, while  $\text{H}_3\text{PO}_4$  resulted in the lowest adsorption capacity of the four acids. This trend indicates that HCl is the most effective activating agent for enhancing the surface properties of sunflower-derived activated carbon, likely due to its ability to remove impurities, increase surface area, and introduce favorable surface functional groups for adsorption. In contrast, the weaker performance of  $\text{H}_3\text{PO}_4$  may be related to less effective pore development or differences in the types of surface functionalities introduced. If you'd like, I can also add a scientific explanation linking these results to pore structure development and surface chemistry changes caused by each acid. That would make it suitable for direct inclusion in a research paper [27–28].

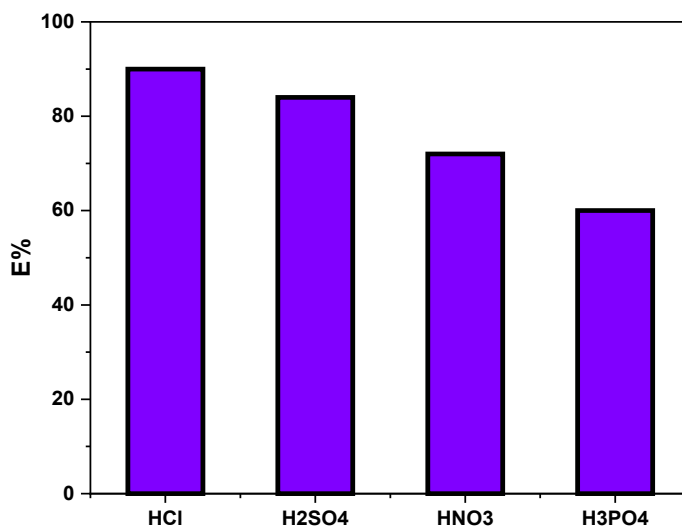


**Figure 9.** Effect of different chemical activating agents—HCl, H<sub>2</sub>SO<sub>4</sub>, HNO<sub>3</sub>, and H<sub>3</sub>PO<sub>4</sub>

### 2.13. Effect of carbonization temperature on adsorption efficiency

Figure 10 illustrates the influence of carbonization temperature on the adsorption efficiency (E%) of sunflower seed shell-derived carbon. Four temperatures were evaluated: 200°C, 300°C, 400°C, and 500°C. The data reveal a non-linear trend in dye removal efficiency as the temperature increases. At 200°C, the adsorption efficiency was approximately 68%, indicating that partial thermal decomposition and limited pore development had occurred. The highest efficiency (92%) was achieved at 300°C, suggesting that this temperature provides optimal conditions for carbonization—maximizing pore formation, surface area, and retention of surface functional groups critical for dye adsorption. At 400°C, the efficiency dropped slightly to around 78%, possibly due to the degradation of some functional groups that are essential for adsorbate interaction. A sharp decline in efficiency to 30% was observed at 500°C, likely due to excessive carbon burnout, pore collapse, or significant loss of active surface sites, which severely reduce the material's adsorptive capacity. These results highlight 300°C as the optimal activation temperature, balancing surface area enhancement and chemical functionality retention. Overheating beyond this point diminishes performance, underscoring the importance of precise temperature control in biochar preparation for environmental applications [29-30].

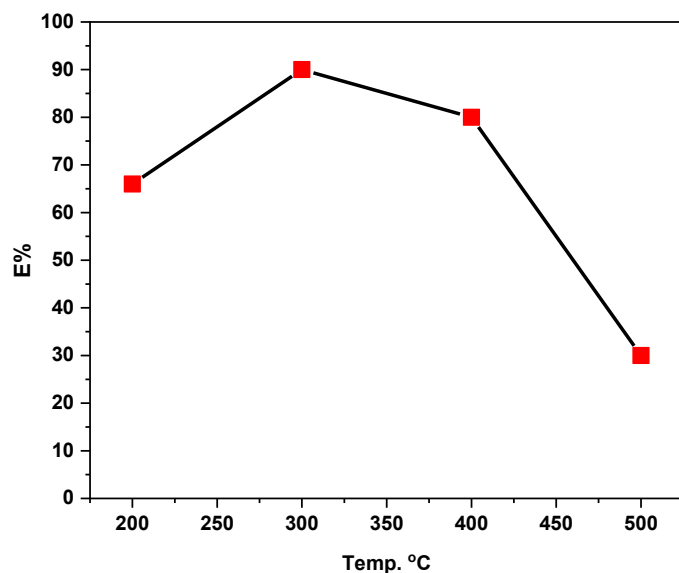


**Figure 10.** Effect of Carbonization Temperature on Adsorption Efficiency

### 3. Effect of different parameters affecting adsorption

#### 3.1. Effect of contact time

The effect of contact time on the adsorption efficiencies of Acid Yellow, Acid Red, Reactive Black, and Reactive Yellow dyes at optimum conditions (initial concentration of dyes 100 mg/L, adsorption dosage 0.08 g, pH 6, contact time 60 min) is shown in Figure 11. All dyes exhibited a biphasic adsorption pattern: an initial rapid uptake followed by a slower approach to equilibrium. The rapid phase is attributed to the abundance of available active sites on the adsorbent surface, while the slower phase reflects site saturation and the establishment of adsorption–desorption equilibrium. **Acid Yellow** achieved the highest removal efficiency, reaching ~90% within the first 20 min and stabilizing at **94%** by 40 min. The high and rapid uptake suggests strong electrostatic interactions and high affinity between Acid Yellow molecules and the adsorbent surface(16). **Acid Red** also showed a high adsorption rate, attaining ~85% efficiency within 30 min and reaching **88%** at equilibrium. The slightly lower efficiency compared to Acid Yellow may be due to differences in molecular size or steric hindrance that limit full surface coverage. **Reactive Black** exhibited a slower adsorption rate, achieving ~80% efficiency at 40 min and stabilizing near **82%**. This slower approach to equilibrium may be related to its larger molecular structure, which could hinder diffusion into the adsorbent pores. **Reactive Yellow** showed the lowest performance, with a maximum removal of ~68% at 40 min. The reduced efficiency likely results from weaker adsorption forces or unfavorable molecular geometry, which reduces the extent of surface coverage. The observed variations in adsorption performance can be attributed to differences in dye molecular size, charge distribution, and chemical structure, all of which influence the interaction strength with the adsorbent. These findings highlight that while the adsorbent exhibits high efficiency for cationic dyes such as Acid Yellow and Acid Red, the removal of larger or less interactive dye molecules, such as Reactive Yellow, remains comparatively limited [26].

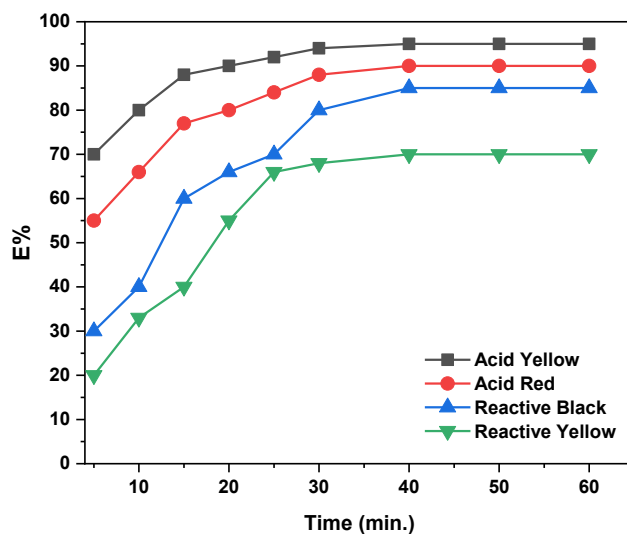


**Figure 11.** Effect of contact time on the adsorption efficiencies of Acid Yellow, Acid Red, Reactive Black, and Reactive Yellow dyes (initial concentration of dyes 100 mg/L, adsorption dosage 0.08 g, pH 6, contact time 60 min)

#### 3.2. Effect of pH

Figure 12 illustrates the effect of pH on the removal efficiency (E%) of four dyes—Reactive Yellow, Reactive Black 5, Acid Red, and Acid Yellow—using the tested adsorbent. Reactive Yellow: This dye shows the most significant decrease in removal efficiency with increasing pH. The E% drops sharply from ~50% at pH 2 to nearly 0% at pH 10. This suggests that adsorption is strongly favoured under acidic conditions, likely due to electrostatic attraction between the positively charged adsorbent surface and the anionic dye molecules, which diminishes at higher pH values as the surface charge becomes negative. Reactive Black 5: Initially, at pH 2, the E% is around 65%, decreasing steadily to ~30% at pH 10. Although the decline is less abrupt than that of Reactive Yellow, the exact mechanism applies—reduced electrostatic attraction at alkaline pH values. Acid Red: The removal efficiency starts high (~85–90%) at pH 2 and remains above 70% up to pH 6, but then drops more markedly to ~50% at pH 10. This indicates that Acid Red adsorption is more tolerant to pH changes than Reactive dyes, though the reduction still influences it in electrostatic interactions at higher pH. Acid Yellow: This dye demonstrates the highest stability against pH changes. Removal efficiency is ~90% at pH 2 and remains above 70% even at pH 10, suggesting strong adsorption through mechanisms beyond simple electrostatic attraction—possibly hydrogen bonding and hydrophobic interactions. All dyes exhibit higher adsorption under acidic conditions due to favorable electrostatic forces. Reactive dyes are more sensitive to pH changes, showing sharper declines in efficiency, whereas acid dyes—especially Acid Yellow—maintain higher performance across the pH range, indicating stronger or more diverse binding mechanisms [16] [24].

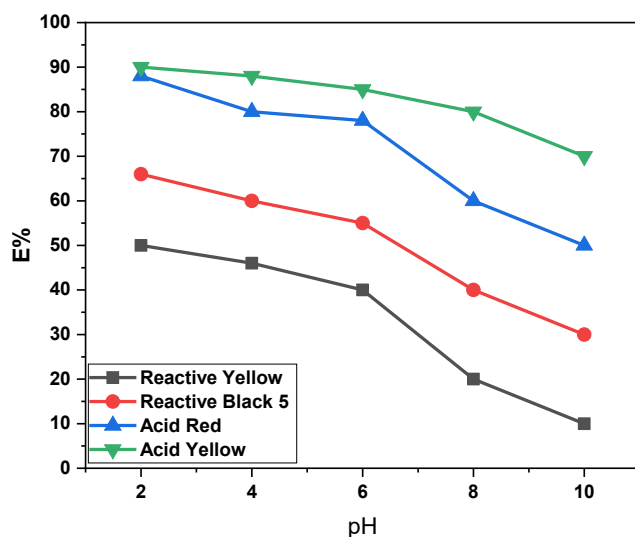


**Figure 12.** Effect of pH solution on to removal dyes by activated carbon ( initial concentration of dyes 100 mg/L , adsorption dosage 0.08 g, contact time 60 min)

### 3.3. Adsorption efficiency of sunflower seed husks for different dyes

Figure 13 illustrates the adsorption efficiency (E%) of sunflower seed husks for four industrial dyes: Reactive Yellow, Reactive Black, Acid Red, and Acid Yellow. The data demonstrate variation in removal efficiency depending on the dye structure and interaction with the adsorbent surface [31].

Acid Yellow exhibited the highest adsorption efficiency at approximately 82%, indicating a strong affinity between the dye and functional groups on the husk surface. Reactive Black exhibited a high removal efficiency of approximately 78%, indicating effective adsorption likely due to  $\pi-\pi$  interactions and electrostatic forces. Reactive Yellow exhibited a moderate adsorption efficiency of roughly 60%, indicating a moderate interaction with the surface sites of the husks. Acid Red recorded the lowest adsorption efficiency, at approximately 43%, which may be attributed to weaker molecular interactions or steric hindrance limiting

access to the active sites. These results confirm that sunflower seed husks can serve as an efficient and eco-friendly adsorbent, particularly for Acid Yellow and Reactive Black dyes, and that adsorption performance is dye-dependent [13] [32].

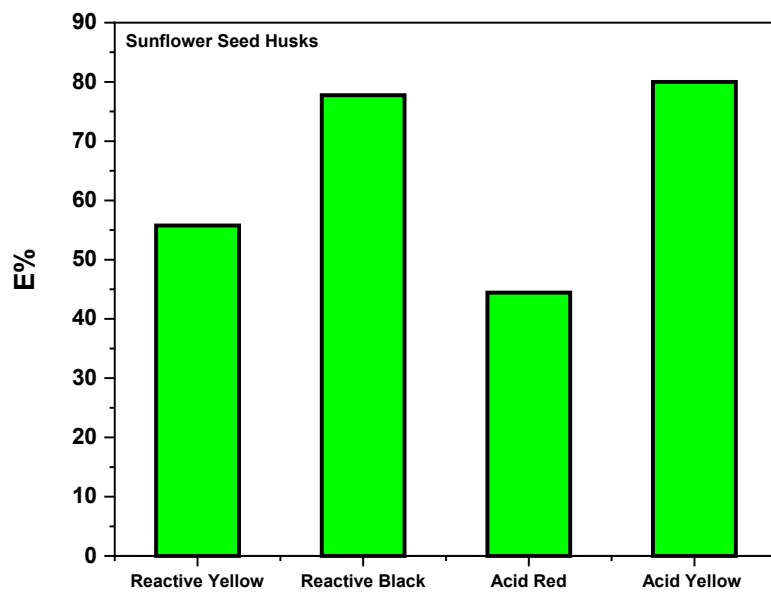


**Figure 13.** Adsorption Efficiency of Sunflower Seed Husks for Different Dyes( initial concentration of dyes 100 mg/L , adsorption dosage 0.08 g, pH 6, contact time 60 min)

#### 3.4. Activated Carbon from Sunflower Seed Shells for the Adsorption of Industrial Dyes

Figure 14 shows the E (%) of industrial dyes Reactive Yellow, Reactive Black, Acid Red and Acid Yellow by ACSSS( initial concentration of dyes 100 mg/L , adsorption dosage 0.08 g, pH 6, contact time 60 min) . These values confirm a remarkable improvement in dye removal efficiency compared to the raw biomass, indicating the role of chemical activation in increasing surface area, porosity, and the presence of active sites. Among them, Acid Yellow exhibited the most significant removal efficiency (~98%) due to the firm adsorption of the dye molecules onto the surfaces of the activated carbon. The adsorptive behaviour can be mainly described by electrostatic attraction and adsorption by surface complexation. The adsorption percentage of Acid Red was approximately 93 %, indicating that efficient binding by  $\pi-\pi$  interactions and oxygen-containing functional groups occurred [28] [33].

Reactive Black exhibited a high efficiency (~87%), indicating good uptake, which could be attributed to its sulfonated nature and planar aromatic rings. The efficiency of Reactive Yellow was slightly lower but still high (approximately 72%) compared to Reactive Black, suggesting a good, albeit relatively moderate, adsorption capacity. These findings demonstrated the high adsorption capacity of the activated carbon towards raw sunflower seed husks. They revealed that it could be used as a low-cost, eco-friendly, and highly effective adsorbent for dye-dirty wastewater [34-35].

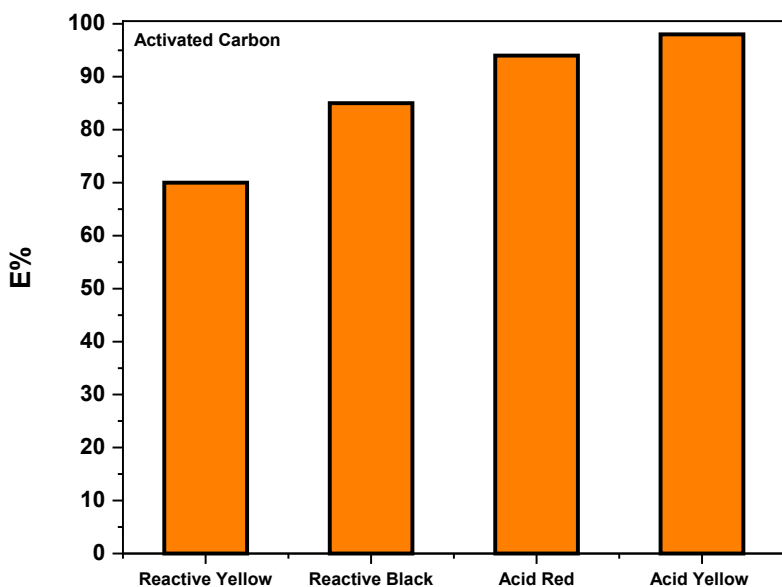


**Figure 14.** Activated Carbon from Sunflower Seed Shells for the Adsorption of Industrial Dyes ( initial concentration of dyes 100 mg/L , adsorption dosage 0.08 g, pH 6, contact time 60 min)

## 4. Conclusion

In this study, sunflower seed shells were investigated as a low-cost and environmentally friendly adsorbent for the removal of hazardous industrial dyes, including Reactive Yellow, Reactive Black 5, Acid Red, and Acid Yellow 23, from aqueous solutions. The biomass was subjected to chemical activation using various acids (HCl, H<sub>2</sub>SO<sub>4</sub>, H<sub>3</sub>PO<sub>4</sub>, and HNO<sub>3</sub>), with hydrochloric acid (HCl) proving to be the most effective based on structural and adsorption performance. Following acid activation, the shells were thermally carbonized at temperatures ranging from 200°C to 500°C, with optimal activation observed at higher temperatures, enhancing surface porosity and functional group exposure. The improved performance of the activated carbon is attributed to the increased surface area, functional group density, and pore volume resulting from acid treatment and carbonization. These improvements facilitated stronger interactions between the adsorbent and dye molecules through electrostatic forces, hydrogen bonding, and  $\pi$ - $\pi$  stacking. In conclusion, acid-activated sunflower seed shells are an efficient, sustainable, and cost-effective adsorbent for treating wastewater contaminated with dyes. Their high removal capacity, especially for acidic and reactive dyes, demonstrates their potential for practical applications in industrial effluent management and environmental remediation.

## Conflict of interest

The authors declare no conflict of interest

## References

1. Rahul, Jindal R (2024); Efficient removal of toxic dyes malachite green and fuchsin acid from aqueous solutions using Pullulan/CMC hydrogel. *Polymer*.307:127203: <https://doi.org/10.1016/j.polymer.2024.127203>.
2. Saeed A, Sharif M, Iqbal M (2010); Application potential of grapefruit peel as dye sorbent: Kinetics, equilibrium and mechanism of crystal violet adsorption. *Journal of Hazardous Materials*.179(1):564-572 :<https://doi.org/10.1016/j.jhazmat.2010.1003.1041>.
3. Aljeboree AM, Alkaim AF, Loay A, Algburi HM (2019); Photocatalytic degradation of textile dye crystal violet wastewater using zinc oxide as a model of pharmaceutical threat reductions. *Journal of Global Pharma Technology*.11(2):138-143.
4. Refaas AMA, Al-Robayi EM, Alkaim AF (2023); Effect of Ag Doping on ZnO/V2O5Nanoparticles as a Photo Catalyst for the Removal of Maxillion Blue (GRL) Dye. *Asian Journal of Water, Environment and Pollution*.20(5):25-31.

5. Salunkhe B, Schuman TP (2021); Super-Adsorbent Hydrogels for Removal of Methylene Blue from Aqueous Solution: Dye Adsorption Isotherms, Kinetics, and Thermodynamic Properties. *Macromol.* 1(4):256-275: <https://doi.org/10.3390/macromol1040018>.
6. Shen Y, Li B, Zhang Z (2023); Super-efficient removal and adsorption mechanism of anionic dyes from water by magnetic amino acid-functionalized diatomite/yttrium alginate hybrid beads as an eco-friendly composite. *Chemosphere.* 336:139233: <https://doi.org/10.1016/j.chemosphere.132023.139233>.
7. Shirasath SR, Patil AP, Bhanvase BA, Sonawane SH (2015); Ultrasonically prepared poly(acrylamide)-kaolin composite hydrogel for removal of crystal violet dye from wastewater. *Journal of Environmental Chemical Engineering.* 3(2):1152-1162: <https://doi.org/10.1016/j.jece.2015.1104.1016>.
8. Hussein UAR, Abd S, Al-Mashhadani ZI, Abid FM, Aljeboree AM, Alkaim AF (2025); Research article Sustainable removal of amoxicillin and tetracycline from aqueous media using Pine-Leaf derived activated carbon: Adsorption performance and regeneration potential. *Applied Chemical Engineering.* 8(2).
9. Alaadin MA, Hammood GA, Adday ST, Hussein AH, Nouri AH (2025); Synthesis of carbon nanoparticles from glucose, evaluation of their phenol adsorption capacity, and study their potential as drug delivery systems for treating human pancreatic cancer cells. *Applied Chemical Engineering.* 8(3).
10. Shah SS, Ramos B, Teixeira AC. Adsorptive Removal of Methylene Blue Dye Using Biodegradable Superabsorbent Hydrogel Polymer Composite Incorporated with Activated Charcoal. *Water* [Internet]. 2022; 14(20).
11. Sharma S, Sharma G, Kumar A, AlGarni TS, Naushad M, Alothman ZA, Stadler FJ (2021); Adsorption of cationic dyes onto carrageenan and itaconic acid-based superabsorbent hydrogel: Synthesis, characterization and isotherm analysis. *Journal of Hazardous Materials.* 421:126729 :<https://doi.org/10.1016/j.jhazmat.122021.126729>.
12. Aljeboree AM (2019); Adsorption and removal of pharmaceutical riboflavin (RF) by rice husks activated carbon. *International Journal of Pharmaceutical Research.* 11(2):255-261.
13. Wei J, Yan L, Zhang Z, Hu B, Gui W, Cui Y (2023); Carbon nanotube/Chitosan hydrogel for adsorption of acid red 73 in aqueous and soil environments. *BMC Chemistry.* 17(1):104.
14. Aljeboree AM, Alkaim AF (2019); Comparative removal of three textile dyes from aqueous solutions by adsorption : As a model (corn-cob source waste) of plants role in environmental enhancement. *Plant Archives.* 19(1):1613-1620.
15. Thakur S, Chaudhary J, Thakur A, Gunduz O, Alsanie WF, Makatsoris C, Thakur VK (2022); Highly efficient poly(acrylic acid-co-aniline) grafted itaconic acid hydrogel: Application in water retention and adsorption of rhodamine B dye for a sustainable environment. *Chemosphere.* 303:134917.
16. Thamer BM, Al-Aizari FA, Abdo HS (2023); Activated Carbon-Incorporated Tragacanth Gum Hydrogel Biocomposite: A Promising Adsorbent for Crystal Violet Dye Removal from Aqueous Solutions. *Gels.* 9(12).
17. Thamer BM, Aldalbahi A, Moydeen A M, El-Newehy MH (2020); In Situ Preparation of Novel Porous Nanocomposite Hydrogel as Effective Adsorbent for the Removal of Cationic Dyes from Polluted Water. *Polymers.* 12(12):3002; <https://doi.org/10.3390/polym12123002>.
18. Thamer BM, Shaker AA, Abdul Hameed MM, Al-Enizi AM (2023); Highly selective and reusable nanoadsorbent based on expansive clay-incorporated polymeric nanofibers for cationic dye adsorption in single and binary systems. *Journal of Water Process Engineering.* 54:103918: <https://doi.org/10.1016/j.jwpe.102023.103918>.
19. Thombare N, Mishra S, Siddiqui MZ, Jha U, Singh D, Mahajan GR (2018); Design and development of guar gum based novel, superabsorbent and moisture retaining hydrogels for agricultural applications. *Carbohydrate Polymers.* 185:169-178: <https://doi.org/10.1016/j.carbpol.2018.1001.1018>.
20. Tian Y, Abed AM, Aljeboree AM, Mohammed HT, Izzat SE, Zare MH, Kotb H, Sarkar SM (2022); Green process of fuel production under porous  $\gamma$ -Al<sub>2</sub>O<sub>3</sub> catalyst: Study of activation and deactivation kinetic for MTD process. *Arabian Journal of Chemistry.* 15(12).
21. Aljeboree AM, Alkaim AF (2024); Studying removal of anionic dye by prepared highly adsorbent surface hydrogel nanocomposite as an applicable for aqueous solution. *Scientific Reports.* 14(1).
22. Tyagi R, Dangi D, Sharma P (2024); Optimization of Hazardous Malachite Green Dye Removal Process Using Double Derivatized Guar Gum Polymer: A Fractional Factorial L9 Approach. *Sustainable Chemistry for Climate Action:* 100043 :<https://doi.org/10.1016/j.scca.102024.100043>.
23. Aljeboree AM, Hasan IT, Al-Warthan A, Alkaim AF (2024); Preparation of sodium alginate-based SA-g-poly(ITA-co-VBS)/RC hydrogel nanocomposites: And their application towards dye adsorption. *Arabian Journal of Chemistry.* 17(3).
24. Ullah N, Ali Z, Khan AS, Adalat B, Nasrullah A, Khan SB (2024); Preparation and dye adsorption properties of activated carbon/clay/sodium alginate composite hydrogel membranes. *RSC Advances.* 14(1):211-221.
25. Aljeboree AM, Hussein FH, Alkaim AF (2019); Removal of textile dye (methylene blue mb) from aqueous solution by activated carbon as a model (corn-cob source waste of plant): As a model of environmental enhancement. *Plant Archives.* 19:906-909.
26. Usmanova GS, Latypova LR, Yusupova AR, Mustafin AG (2025); Preparation of Copolymers Based on Aniline and 2[2-chloro-1-methylbut-2-en-1-yl]Aniline and Their Application for the Removal of Methyl Orange from

Aqueous Solutions. *Journal of Polymers and the Environment*. 33(3):1585-1600: <https://doi.org/10.1007/s10924-10024-03419-x>.

- 27. Abdelmajid R, Rachid L, Stiriba S-E, El Haddad M (2017); The potential use of activated carbon prepared from *Ziziphus* species for removing dyes from waste waters. *Applied Water Science*. 7.
- 28. Pathania D, Sharma S, Singh P; Removal of methylene blue by adsorption onto activated carbon developed from *Ficus carica* bast. *Arabian Journal of Chemistry*. 10:S1445-S1451.
- 29. Aljeboree AM, Radi N, Ahmed Z, Alkaim AF (2014); The use of sawdust as by product adsorbent of organic pollutant from wastewater: Adsorption of maxilon blue dye. *International Journal of Chemical Sciences*. 12(4):1239-1252.
- 30. Vahid B, Hossein P, Mohammad SA, Dariush S, Siamak J (2023); Synthesis and characterization of bio-nanocomposite hydrogel beads based on magnetic hydroxyapatite and chitosan: a pH-sensitive drug delivery system for potential implantable anticancer platform. *Polymer Bulletin* 23:1223: <https://doi.org/10.1007/s00289-0023-05072-00281>.
- 31. Mulla B, Ioannou K, Kotanidis G, Ioannidis I, Constantinides G, Baker M, Hinder S, Mitterer C, Pashalidis I, Kostoglou N, Rebholz C. Removal of Crystal Violet Dye from Aqueous Solutions through Adsorption onto Activated Carbon Fabrics. C [Internet]. 2024; 10(1).
- 32. Weber WJJ, Morris JC (1963); Kinetics of Adsorption on Carbon from Solution. *Journal of the Sanitary Engineering Division*. 89:31-59.
- 33. Zhokh A, Strizhak P (2019); Crossover between Fickian and non-Fickian diffusion in a system with hierarchy. *Microporous and Mesoporous Materials*. 282:22-28: <https://doi.org/10.1016/j.micromeso.2019.1003.1016>.
- 34. Xinyou M, Lan W, Shiqing G, Yanyan D, Yunqing Z, Chuanyi W, Eric L (2018); Synthesis of a three-dimensional network sodium alginate–poly(acrylic acid)/attapulgite hydrogel with good mechanic property and reusability for efficient adsorption of Cu<sup>2+</sup> and Pb<sup>2+</sup>. *Environmental Chemistry Letters*. 16:653–658.
- 35. Xisto MR, Damacena DHL, de Araújo FP, Alves D, Honorio LMC, Peña-Garcia R, Almeida L, de Oliveira JA, Furtini MB, Osajima JA (2024); Biopolymer Gellan-Gum-Based TiO<sub>2</sub>: A Green Alternative Photocatalyst Approach for Removal of Pollutants. *Water*. 16(2):315.